Numerical simulation of the de-bonding phenomenon in small diameter grouted anchors

Mohamed Askar
Sogreah Gulf FZCO, Dubai, UAE
Ahmed Fahmy
30 Forensic Engineering, Toronto, Canada

ABSTRACT
Grouted ground anchors are consistently used in practice to stabilize and support a wide range of structures. While a considerable number of existing studies describe the behavior of larger diameter anchors, less attention was given to smaller diameter ones. In this paper, evaluation of the load transfer mechanism of small diameter grouted anchors is presented based on the results of the full-scale field load tests presented by Bingham et al. (2010) in their article titled "Load Transfer Mechanism of Small-Diameter Grouted Anchors". Additionally, a two-dimensional Finite Element FE model was created using the commercial software Geoslope - SIGMA/W (Geo-Slope International Ltd, 2012) to simulate the reported field tests to further understand the load transfer mechanism during the different loading stages. Showing good agreement with the field instrumentation measurements, the model clearly illustrated the progression of the load transfer mechanism along the strand-grout-soil interfaces up to failure. Findings of model highlighted the significant effect of the de-bonding phenomenon, controlling the anchor performance at various loading phases. Based on the discussion of Bingham et al. (2010) reported results, and the findings of the FE simulations, practical recommendations to monitor and control the anchor de-bonding phenomenon during load tests are given.

RESUME
Les ancrages injectés sont continuellement utilisés dans la pratique pour stabiliser et soutenir différents types de structures. Tandis qu'un grand nombre d'études existantes décrivent le comportement des ancrages de grand diamètre, moins d'études ont abordés celui des ancrages de faible diamètre. Dans cet article, l'évaluation du mécanisme de transfert de charge des ancrages injectés de faible diamètre est présentée sur la base des résultats des essais de chargement en vrai grandeur effectués in situ et présentés par Bingham et coll. (2010) dans leur article intitulé ""Load Transfer Mechanism of Small-Diameter Grouted Anchors". De plus, une modélisation 2D par éléments finis a été créée en utilisant le logiciel commercial Geoslope - SIGMA / W (Geo-Slope International Ltd, 2012) pour simuler les essais in situ afin de mieux comprendre le mécanisme de transfert de charge durant les différentes étapes de chargement. Le modèle montre une bonne concordance avec les mesures in situ ainsi qu'il a clairement montré la progression du mécanisme de transfert de charge le long des interfaces fil-coulis-sol jusqu'à la rupture. Les résultats du modèle ont soulignés l'effet important du phénomène de décollement, contrôlant la performance de l'ancrage à différentes étapes de chargement. Basé sur la discussion des résultats présentée par Bingham et coll. (2010) et sur les résultats de la modélisation par éléments finis, des recommandations pratiques pour surveiller et contrôler le phénomène de décollement des ancrages pendant les tests de charge sont présentées.

1 INTRODUCTION

A variety of ground anchor configurations currently exist in literature making anchors a viable support system to sustain different loading conditions (Fahmy, 2013). Generally, six categories of anchors are used in industry: plate anchors, helical anchors, anchor piles, drilled shafts, direct embedment anchors, and grouted anchors (Das, 2012). Depending on the application, anchors may be subjected to complex loading cases (Fahmy, 2013). For instance, if used as foundations of transmission towers, the applied forces are primarily uplift, whereas in shoring systems the anchors may be subjected to lateral loads (Merrifield et al., 2013).

As for grouted anchors, of main concern here, they may be defined as structural elements installed in grout filled holes in rock or soil and are able to transfer the applied tensile stresses to the surrounding ground (FHWA, 1999).

A considerable number of studies exist in literature evaluating the performance of grouted anchors in different soil conditions (Kim, 2003; Ostermayer and Scheele, 1978; Johnston and Ladanyi, 1972; Evangelista and Sapio, 1978). Less attention was, however, given to smaller sized ones.

In an effort to better evaluate the load transfer mechanism of small diameter grouted anchors, Bingham et al. (2010) presented the results of full-scale field load testing of seven multi-strand anchors of 9.525 mm diameter. The tests were carried out at the Bonneville Locks on the Columbia River by L.R. Squier Associates (1986) (Figure 1).

Figure 1: S Satellite view of the test site location (©2017 Google)

The following points were noted by Bingham et al. (2010):

- Anchor loading may generate compressive and tensile stresses in the bonded zone, with the compressive stresses in grout possibly extending beyond the bonded length of the anchor;
- Compressive stresses are directly proportional to the applied loads;
- A number of factors may control the occurrence of compressive stresses in the bonded zone, including the anchors boundary (i.e. restraining) conditions and the possibility of suppressed dilation;
- The applicability of traditional straight shaft resistance assumptions depends on the dilation conditions;
- The location/extent of the unbounded portion may affect anchor capacity. Specifically, Bingham et al. (2010) believed that moving the unbonded portion of the anchor into the load zone may result in "*higher anchor performance*." We suspect, however, that it could lead to an uncontrolled performance depending on a number of factors including the cracking or de-bonding of the anchor grout mass. Further discussion of this latter point is presented in the following sections.

3 SUBSURFACE CONDITIONS

The anchors were installed and tested on a site on the Columbia River East of Portland, Oregon. The geology of the site comprises a heterogeneous mix of materials comprising from as small as silt particles to large boulders. Classification of the subject soils is not available to us at the time of writing this paper.

It should be noted that the area had previously experienced a major landslide. The material displaced in the slide was categorized as slide debris (SD), with a mixture of angular rock fragments to large boulders contained in a clay-rich matrix. The Colombia River erosion also contributed to the formation of soil layers defined as reworked slide debris (RSD). Nevertheless, the soil mechanical properties were not introduced by Bingham et al. (2010).

The subsurface cross-section illustrated in Figure 2 and adopted by Bingham et al. (2010) is based on L.R. Squier Associates (1986) reported profile.

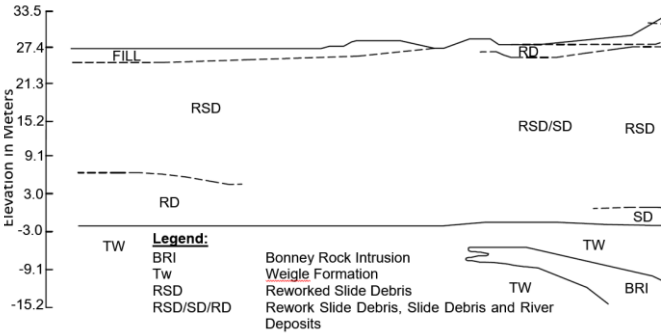

Figure 2: Stratigraphic cross section at Tiebacks No. 1 and No. 2 test site (Reproduced after Bingham et al. (2010))

4 ANCHOR CONFIGURATION

Three anchors were installed in boreholes of 187 mm diameter and were then tremie grouted. The grout measured strengths (Table 1) are based on 10 to 13-day compressive tests. All tested anchors had a total of 17 strands, 7-wire, with 15.24 mm. outside diameter. The 30.5 m unbonded sections were inclined by 20 to 23 degrees from the horizontal (Bingham et al., 2010).

Electrical resistance strain gauges were used to instrument the tested anchors and to evaluate the load transfer mechanism during the different loading stages. The gauges were mounted on PVC pipe sections. Each tendon was instrumented using 3 instrumentation pipes, each fitted with five gauges uniformly distributed and placed as close to the soil-grout interface as practically as attainable. Further details about the anchors' instrumentation is provided by Bingham et al. (2010).

A rotary percussion drill was used to install the anchors to account for the presence of boulders within the soil matrix. The design unbonded zones were cased with standard well casing. The anchor surface gauge grout pressures ranged between 138 to 414 kPa.

In this paper, the results of two tested tiebacks (Tiebacks No. 1 and No. 2) are analysed and numerically simulated, knowing the third tieback was reported as a failed test. The installation data of the three tiebacks are summarized in Table 1.

Table 1: Anchor Tieback Installation Data (Bingham, Mikkelsen, & Petersen, 2010)

Tieback No.	Bond Length (m)	Approximate Grout Volume (m^3)	Theoretical Hole Volume (m^3)	Static Grout Pressure (kPa)	Grout Compressive Strength f_c(MPa)
1	6.1	0.63	0.72	285	30.8
2	12.2	1.54	0.88	333	30.8
3	18.3	1.63	1.05	389	31.0

5 FIELD TESTING - LOADING PROTOCOL

The anchors were loaded and unloaded in a repeated fashion. Creep tests were then applied to the anchors. Maximum field test loads are summarized in Table 2. It should be noted that for Tieback No. 2, two strands were damaged during installation and therefore, the maximum testing load was reduced to avoid overstressing the remaining strands.

Table 2: Summary of field test results after Bingham et al. (2010)

Tieback Number	Maximum Test Load (kN)	Installed Bond Length (m)	Average Load Transfer Length (m)
1	3914	6.1	7.5
2	3647	12.2	7.6
3	3914	18.3	7.2

6 LOADING PROTOCOL AND DE-BONDING OBSERVATIONS

As shown in Table 2, the maximum anchor test load approached 4000 kN.

The load transfer mechanism in grouted anchors generally depends on stress reversal, typically observed at the interface of the unbonded and bonded portions of anchors (Briaud et al., 1998). This was shown in the test results of Tieback No. 2, later discussed in Section 9, where the gages readings showed a fluctuation between tensile and compressive stresses at/around the interface between the unbonded and bonded portions at the different loading stages. This was not the case for Tieback No. 1 where the location of the stress reversal zone varied with loading steps (Figure 3). Specifically, the observed location of the stress reversal moved towards the tip of the tieback with the increase of test loads. This suggests a tendon de-bonding occurring at relatively early stages of loading and continued until the end of testing.

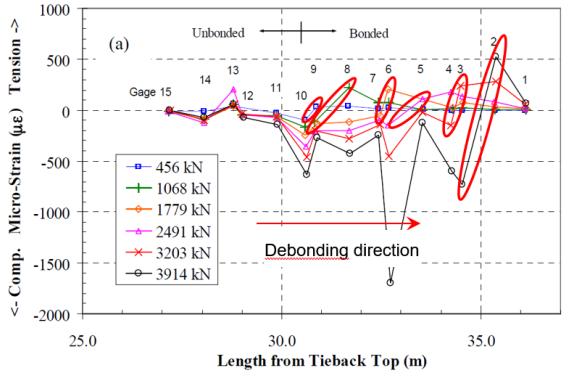

Figure 3: Tieback No. 1 strain measurement along the anchor length - After L.R. Squier Associates (1986)

As for the de-bonding phenomenon, Petros P. (1991) reported that it is usually associated with high capacity anchors (e.g., of design loads exceeding 200 tons metric, where progressive cracking of the grout starts at the point of increasing the load, resulting in the loss of friction/adhesion along the critical bonded zone. Similar behavior was observed by Muller (1996) on test anchors loaded to 220 tons

In addition of the high loading, one of the reasons that may result in grout cracking is the density of the tendons within the borehole. A minimum of 5 mm spacing between strands is generally required to ensure proper tendon-grout bond (BS 8081, 2015). Similarly, FHWA (1999) recommends a minimum spacing between strands ranging between 6 and 13 mm. We are not aware at the time of writing this paper whether the anchor configurations fulfilled this condition or not.

7 NUMERICAL SIMULATION

Two-Dimensional finite element simulations of the field tests presented by Bingham et al. (2010) were developed using the commercial software package Geoslope - SIGMA/W (Geo-slope International Ltd, 2012). The analyses were carried out to further understand the load transfer mechanism during the load testing and to evaluate the de-bonding effect, especially in Tieback No. 1.

A mix of 4-noded quadrilateral and 3-noded triangular elements were used to discretize the problem. The developed model comprised a total of 2412 elements. An excerpt of the developed mesh is shown in Figure 4.

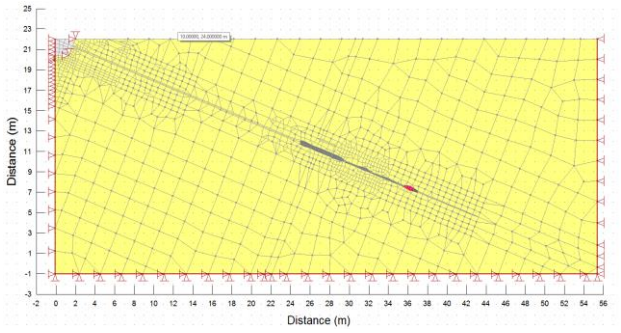

Figure 4: Mesh Arrangement (Geo-Slope International Ltd 2012)

The model boundaries were extended vertically and laterally to the distances shown in Figure 4 to delineate any effects on the model results. Sensitivity analysis was carried out to determine the suitable mesh size and the expected grout bulb shape. Further refinement around the anchor bonded length was necessary to ensure the model convergence and accuracy.

The anchor was wished in place in the RSD formation. The RSD layer was modeled using an elastic, perfectly-plastic relationship (Mohr-Coulomb model), while the interface and grout materials were modeled using a linear elastic model. The soil mechanical properties considered in the analysis were based on Mosher's study (1990) conducted in similar subsurface conditions and were verified using the results of anchor field load test results (Bingham et al., 2010). The mechanical properties of the soil and anchors are summarized in Table 3 and Table 4, respectively. The value of the angle of internal friction lies within the typical range for dense, coarse granular material (Bowles, 1996).

Structural bar elements were used to model the unbonded length of the anchor, carrying axial loads only. The bonded (zones) were simulated using structural beam elements aligned with the surrounding soil mass. The stiffness and cross-sectional area of the anchoring system was divided by a spacing of 3 m to convert the 3D problem to an equivalent 2D (plane strain) model. A change in the elastic modulus of the grout bulb was adopted in the analysis, to account for the effect of large strains and the possible development of cracks in the grout body. The change in the grout elastic modulus followed the recommendations of CAN/CSA (2004) for the reduction of concrete member gross inertia due to cracking.

Table 3: Soil and grout mechanical properties considered in the finite element model

Material	RSD	Grout
Unit Weight, γ (kN/m^3)	19.6	24
Young's modulus E' (MPa)	70	(12E03 to 4E04)
Peak angle of internal friction φ_p) (^{o})	45	NA
Cohesion c' (kPa)	0	NA
Dilation Angle ψ (^{o})	3	NA
Poisson's Ratio ν	0.3	0.2

Table 4: Anchor mechanical properties considered in the finite element model

Material	Young's Modulus E' (kPa)	No. of Strands	Area (mm^2)	Poisson's Ratio, ν	Anchor spacing (m)
Tendons (Tieback No. 1)	3x10^8	17	2380	0.15	3
Tendons (Tieback No. 2)	3x10^8	15	2100	0.15	3

8 FINITE ELEMENT - LOADING SEQUENCE

Load testing of two tiebacks was numerically simulated (Tieback No. 1 and Tieback No. 2). An initial calculation step of geostatic stresses was employed to consider the initial in-situ overburden soil stresses. This was followed by a load controlled analysis step, whereby prescribed loading protocol, shown in Table 5, was followed.

The applied forces on the anchors were assigned using a prescribed pre-stressing force in the node to node structural bar element.

Table 5: Loading sequence for the anchor load tests

Loading Step	Applied load (kN)	
	Tieback No. 1	Tieback No. 2
Step 1	456	356
Step 2	1068	1068
Step 3	1779	1779
Step 4	2491	2491
Step 5	3203	3203
Step 6	3914	3647

9 RESULTS AND DISCUSSION

A plot of the deformed mesh showing the displacement contours at the final loading stage of Tieback No. 1 and

Tieback No. 2 are shown in Figure 5 and Figure 6, respectively.

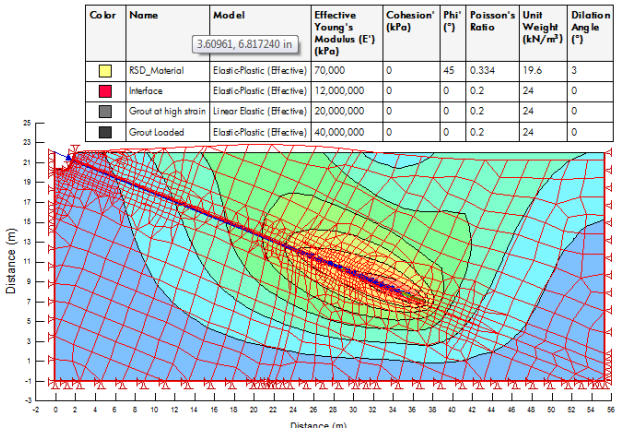

Figure 5: Deformed mesh and displacement contours - Tieback No. 1

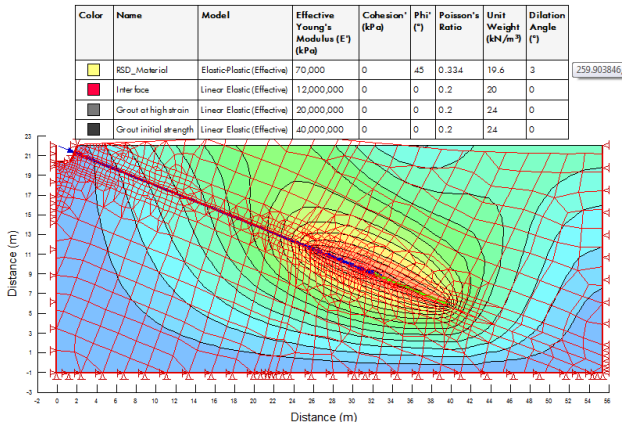

Figure 6: Deformed mesh and displacement contours - Tieback No. 2

The variation of the strain along the anchor bonded zone, found from the finite element model, are shown in Figure 7 and Figure 8 at different applied loading levels for Tiebacks No. 1 and No. 2, respectively. The results show good agreement with the field measurements reported by Bingham et al. (2010). The results show that both compressive and tensile strains were observed in the bonded zone. A change from compressive to tensile stresses was also observed at each loading step.

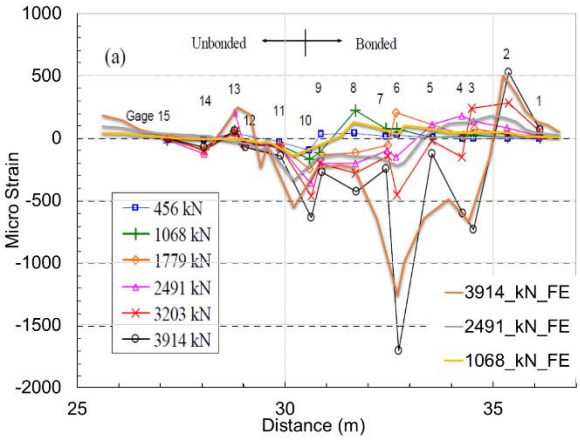

Figure 7: Variation of Micro strain along the Anchor bonded and unbounded lengths, F.E. versus experimental for Tieback 1

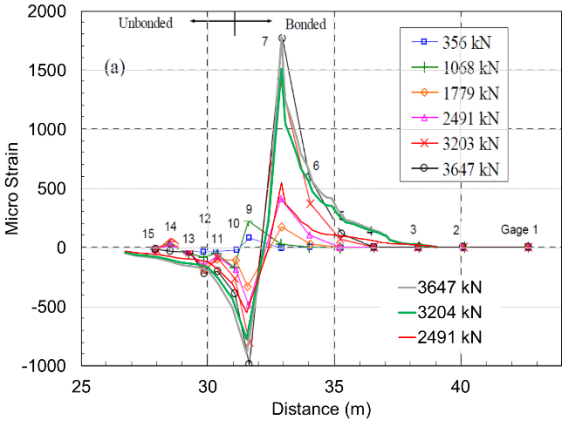

Figure 8: Variation of Micro strain along the Anchor bonded and unbounded lengths, F.E. versus experimental for Tieback 2

The analysis results indicate the effect of de-bonding on the stress transfer behavior in Tieback No. 1, where the micro strains reading showed an irregular behavior along the anchor length. On the other hand, the test results of Tieback No. 2, showed no clear signs of de-bonding. However, cracking of the grout was manifested in the last two loading steps of Tieback No. 2 where the measured micro strains significantly increased in both compression and tension.

The switch between tensile and compressive stresses along the interface reflects the decrease of the effective bond zone. It is believed that the progressive grout cracking with increased loading resulted in this behavior and subsequently de-bonding along the soil-grout interface.

The reported instrumentation measurements do not show clear indications of where the cracks initiated (i.e. within the grout body, at tendon/grout interface…etc). As discussed earlier, the anchors were wished in place and, therefore, we assume that no de-bonding has occurred during anchor installation.

10 CONCLUSIONS

In this paper, finite element simulation of the previously reported anchor field test results by Bingham et al. (2010) was performed. Progression of the developed stresses along the grout-soil interface is thoroughly discussed. Stress reversal along the bonded zone of the anchor was observed depicting a possible de-bonding phenomenon likely resulting from the grout cracking with increased loading. The results of this study highlight the importance of considering the de-bonding phenomenon in the design of anchors, specially highly loaded ones. Monitoring the strain levels in the grouted mass at early loading stage may help identifying and possibly avoiding anchors de-bonding. The use of cracked grouted modulus is believed to be essential for proper modelling of the anchors, specifically at higher loading levels approaching the anchor's structural capacity. More research is needed to further confirm the findings of this study for different loading conditions, anchor configurations, and soil types.

11 REFERENCES

Barley, A. D., & Windsor, C. R. 2000. Recent Advances in Ground Anchor and Grout Reinforcement Technology with Reference to the Development of the Art. *Proceedings of GeoEng2000: International Conference on Geotechnical and Geological Engineering*, Melbourne, Australia, 1: 1084-1094.

Bowles, J. E., 1996. *Foundation analysis and design*, 5th ed., McGraw-Hill, New York, NY, USA

Bingham, J. N., Mikkelsen, E. P., & Petersen, G. L. 2010. Load Transfer Mechanism of Small-Diameter Grouted Anchors. *Earth Retention Conference (ER2010),* ASCE, 1: 196-203.

Briaud J. L., Powers W., & Weatherby D. 1998. Should Grouted Anchors Have Short Tendon Bond Length? .*Journal of Geotechnical and Geoenvironmental Engineering,* 124(2).

BS8081. 2015. *Code of practice for grouted anchors*. British Standards Institution.

Canadian Standard Association. 2004. Design of concrete structure. CAN/CSA-A23.3-04 (R2010)

Das, B. M. 2012. *Earth anchors*, Elsevier, Amsterdam, Netherlands.

Evangelista, A., & Sapio, G. 1978. Behaviour of ground anchors in stiff clays. *Revue Française de Géotechnique*, 3: 39-47.

Fahmy, A. M., de Bruyn, J. R., & Newson, T. A. 2013. Numerical investigation of the inclined pullout behavior of anchors embedded in clay. *Geotechnical and Geological Engineering*, 31(5): 1525-1542.

FHWA. 1999. *Ground anchors and anchored systems*. Geotechnical engineering circular No. 4, Federal Highways Administration, US Department of Transportation, Washington, DC.

Geo-Slope International Ltd. 2012. Stress-Deformation Modeling with SIGMA/W. Calgary, Alberta, Canada: GEO-SLOPE International Ltd.

Google Inc. 2017. Google Earth (Version 7.3.0.3832) [Software]. Retrieved January 2, 2018.

Johnston, G. H., & Ladanyi, B. 1972. Field tests of grouted rod anchors in permafrost. *Canadian Geotechnical Journal*, 9(2): 176-194.

Kim, N. K. 2003. Performance of tension and compression anchors in weathered soil. *Journal of Geotechnical and Geoenvironmental Engineering*, 129(12): 1138-1150.

L.R. Squier Associates. 1986. Phase II Tieback Testing Program Bonneville Navigation Lock. Portland District: US Army Corps of Engineers, Technical report ITL 90-4

Merifield, R. S., Lyamin, A., Sloan, S. W., & Yu, H. S. 2003. Three-dimensional lower bound solutions for stability of plate anchors in clay, *Journal of Geotechnical and Geoenvironmental Engineering,* 129(3): 243-253.

Mosher, R. L., & Knowles, V. R. 1990. Finite Element Study of Tieback Wall for Bonneville Navigation Lock. Department of the Army, Information Technology Laboratory. Vicksburg, Mississippi: US Army Corps of Engineers.

Ostermayer, H., & Scheele, F. 1978. Research on ground anchors in non-cohesive soils. *Revue Française de Géotechnique*, 3: 92-97.